



Synthesis and characterization of rare earth metal and non-metal co-doped TiO₂ nanostructure for photocatalytic degradation of Metronidazole

Khaled Elgendy^{1*}, Ibrahim Elmehasseb², Saleh Kandil^{1,3*}

¹Chemistry Department, Faculty of Science, Zagazig University, Zagazig, Egypt

²Chemistry Department, Faculty of Science, Kafrelsheikh University, 33516Kafrelsheikh, Egypt

³Institute of Nanoscience & Nanotechnology, Kafrelsheikh University, 33516Kafrelsheikh, Egypt

Received 28 March 2019,
Revised 19 April 2019,
Accepted 20 April 2019

Keywords

- ✓ TiO₂ nanoparticles,
- ✓ Metronidazole,
- ✓ Photodegradation,
- ✓ Bandgap,
- ✓ Performance.

*Corresponding author:
el_gendykh@yahoo.com
(Tel. +205169453)

Abstract

The harmful effects resulted from the continuous discharge of pharmaceutical compounds in wastewater led to great problems which require to be rapidly addressed. Herein, doping with rare earth metal Ce and/or nonmetal C, N co-doped TiO₂ has been proved to be excellent tool for improvement of the photocatalytic performance of TiO₂ in the elimination of wastewater pharmaceutical pollutants. In this regard, the TiO₂ nanoparticles have been doped with Ce on one hand and doped with Ce, N, C on the other hand. The photocatalysts were synthesized by sol-gel procedure. The characterization was carried out by FT-IR spectroscopy, XRD, SEM. This doping approach has implications on the optical properties of TiO₂, since the band gap of the TiO₂ nanoparticles was reduced from 3.2 e.V to 2.6 e.V due to the successful introduction of the dopants C, N, and Ce, which is proved by UV-Visible spectroscopy. Furthermore, the photocatalytic activities of the doped-TiO₂ nanoparticles for the degradation of MTZ, as a model of the pharmaceutical compounds have been studied under visible light illumination. The TiO₂ nanoparticles doped with Ce, N and C able to decompose MTZ within 120 min following the pseudo-first order, thus demonstrating higher photocatalytic performance in the degradation of the pharmaceutical pollutants.

1. Introduction

Human and veterinary pharmaceutical antibiotics are used everywhere for both human being and animals [1-5] Owing to high levels of consumption, the drinking and sewage water are contaminated by their residues. These toxins are non-biodegradable, teratogenicity and whole accumulated in the human body [6]. Moreover, the antibiotics lose their viability and stability due to the resulted bacterial resistance [7-9]. Antibiotics residues should be completely removed from wastewater by different means as reported in the literature to save the planet. Physical, chemical and biological techniques were discussed to minimize the potential impacts on the environment [10, 11].

Amongst those techniques, the heterogeneous photocatalytic system in the presence of semiconductor-liquid interface implying great magnificent such as simplest, low-cost, free renewable treatment process, leading to oxidize the water contaminants to affordable CO₂, H₂O and mineral acids. On the other hand, the initiation takes place by the aid of light to promote the generation of huge quantities of hydroxyl radicals ($\cdot\text{OH}$) [12-15]. TiO₂ nanocatalyst is used for detoxification of chemical contaminants including organic pollutants [16].

Sol-gel is an easy and inexpensive technique in controlling the formation of different inorganic nanoparticles at relatively low annealing temperatures with a high yield, and homogeneity. [17-21] In this method, the self-assembly properties of the surfactant, macromolecule or polymers are exploited in controlling the nucleation and growth mechanisms of the inorganic nanoparticles with the precise size and morphologies. TiO₂ is one of those important nanoparticles used for the photocatalytic applications that have been synthesized via this technique. Also sol-gel method gives the ability for introducing of different dopants during the fabrication process.

TiO₂ nanoparticles act as a catalyst and the energy of absorbed photons can generate an effective hydroxyl radical and push photocatalytic oxidation mechanism for complete decomposition of organic pollutants. [22-24].

But the wide bandgap of TiO_2 , make it useful only in UV irradiation, limiting the utilization of TiO_2 in visible light [25-29]. So, improvement of the sensitivity of TiO_2 to visible light becomes an essential target for scientists. [17-20].

Doping by rare earth metals such as Ce becomes an effective method for extension of photoresponse of TiO_2 to visible light irradiation [30]. As it can cause charge separation between electrons and holes by electron trapping, preventing electron-hole recombination. Also doping with nonmetal like C, N can be very applicable in that way and improve the catalyst sensitivity towards visible light [31, 32].

MTZ is one of the most common antibiotics, used for the treatment of infections of anaerobic bacteria.

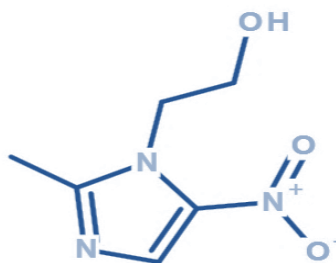


Figure 1: Chemical structure of metronidazole

Besides to its use for human as antibacterial, it is also for weight enhancement to fish. That can illustrate its wide consumption. MTZ is soluble in water, cannot be easily adsorbed on soil, highly mobile and non-biodegradable leading to its accumulation which causes toxic and carcinogenic effects for human through drinking and groundwater [33, 34]. That requires urgent attention to protect the environment and to decrease surface water and groundwater contamination by drug residues via water treatment. Developing novel methods to fully remove antibiotics from wastewater is hence of great significance. It is great if we can completely remove the drug contaminants from water by superior methods. [35-38].

2. Experimental

2.1. Materials

Titanium (IV) butoxide 97%, Cerium nitrate hexahydrate, cetyltrimethylammoniumbromide (CTAB), and citric acid were provided from Sigma Aldrich, USA. Absolute ethanol and Urea were purchased from LOBA-Chemi, India. Metronidazole was purchased from Sigma Pharmaceuticals. Sodium hydroxide was obtained from AppliChem, Germany.

2.2. Synthesis of photocatalysts TiO_2 and Ce-doped TiO_2

Synthesis of TiO_2 nanoparticles by sol-gel method according to published elsewhere [5] with slight modification. Typically, 15 ml of pure Titanium (IV) butoxide solution was dissolved in 20 ml absolute ethanol with vigorous stirring till pale-yellow color obtained. Then the total 35 ml was added wise-batch to the following as-prepared solution: 2 gm of CTAB prepared in 75 ml DDI (0.1 M) citric acid to prevent agglomeration of the network structure. All reaction lasted overnight at controlled temperature, in the same time, 1 wt. % of cerium nitrate hexahydrate in-situ formation to produce Ce-doped TiO_2 , the off-white suspended particles were centrifuged at 6000 RPM for 10 min at each run with repeated washing with mixed solvent. The obtained powder was dried for two days at 70 °C, before calcination at controlled 450 °C and the obtained powder kept prior to use.

2.3. Synthesis of N, C Ce co-doped TiO_2 nanocomposite

For comparison another doping source was introduced. In this regard, ex-situ preparative technique was prepared as well as 1:1 wt. % urea to Ce doped- TiO_2 . Thereto, wise portion was calcined up to 450 °C for 6 hour with ramping 5°/min, then cooling at R.T. The two series nominated Ce-doped- TiO_2 and N, C, Ce co-doped TiO_2 , respectively.

2.4. Instruments

For the synthesis process of nanomaterials, Ultrasonic bath (CB -2500B, China) have been used to give high homogeneity for reacting materials. pH meter (3510 pH meter JENWAY, UK) for adjustment of the medium pH. The resulted yield has been dried in the Oven (MTI Corporation, USA). The crystalline nanoparticles were

obtained by calcination process using Muffle furnace (Up to 1500 °c) Japan. The nanoparticles size and phase was characterized by X-ray Diffraction (XRD - 6000 SHIMADZU, Japan). SEM equipped with (EDX) (JSM IT 100 JEOL, Japan) for studying the surface morphology and EDX to examine the type of resultant atoms. The illumination process was carried out using visible light source (Halogen lamp 500 watt Osrema, japan) and then, band gap and photoresponse of the prepared nanoparticles were examined by UV Spectrophotometer (UV – 2450 SHIMADZU, Japan).

2.5. Photocatalytic evaluation study

In order to investigate the effect of TiO₂ nanoparticles on photocatalytic degradation of MTZ, 10 mg of different prepared catalysts were added to a solution containing 10 μ gram/ml of MTZ. Stir for 30 min to achieve equilibrium between adsorption and desorption on the surface of the catalyst under illumination of visible light using 500 W halogen lamps. The absorbance of MTZ was measured at different times at 320 nm by UV-Visible spectrophotometer

3. Results and discussion

FTIR analysis

The Fourier Transform Infrared Spectroscopy (FTIR) using an FT-IR spectrometer which can study the change in the structure by illustrating the shift in the position of the peaks.

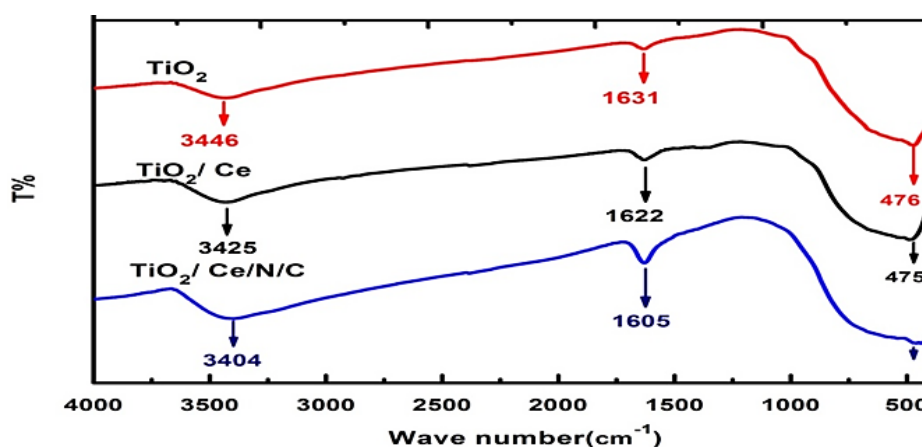


Figure 2: FT-IR spectrum of (a) TiO₂ (b) TiO₂/Ce, and (c) TiO₂/Ce/N/C.

The FT-IR spectroscopy of TiO₂, Ce/TiO₂, and N, C, Ce co-doped-TiO₂ are shown in Fig(2). The spectra of TiO₂ exhibited two peaks at 3446 and 1631 cm⁻¹ ascribed to the stretching and bending vibrations of -OH groups in titanol. The two hydroxyl characteristic peaks were slowly shifted towards 3425 cm⁻¹ and 1622 cm⁻¹ respectively during Ce modified TiO₂; this indicated that the surface activity was enhanced [39]. On the other hand, the clear band at 475 cm⁻¹ proves existence of Ti-O stretching vibration which nearly diminished after introducing of N,C owing to the formation of new bond (N-Ti-O) proving incorporated N,C into Ce/TiO₂ in addition to more shift of two hydroxyl characteristic peaks towards 3404 cm⁻¹ and 1605 cm⁻¹ [40].

XRD analysis

X-ray diffraction represents the crystal phases (101), (004), (200) and (105), (211) for the prepared catalysts bare TiO₂, TiO₂/Ce, and TiO₂/Ce/N/C. The XRD pattern exhibit the different intense peak at (25.05, 37.74, 47.8, 53.82 and 62.4) [41], for TiO₂, Ce doped TiO₂ and TiO₂/Ce/N/C, respectively. The results were emphasized that the synthesized materials are pure crystalline particles [5]. The crystal size has been documented at 10.1 nm, 19 and 25 nm respectively where is calculated from Scherer's equation (Eq. 1):

$$D = k \lambda / \beta \cos \theta \quad (1)$$

Scanning electron microscope (SEM)

The scanning electron microscope figures 4 illustrate the change in particle size, shape, and energy content compared to undoped TiO₂. The characterization by SEM and EDX prove the presence of the doped metal and nonmetals in the lattice of the modified nanocomposites TiO₂/Ce and TiO₂/Ce/N/C

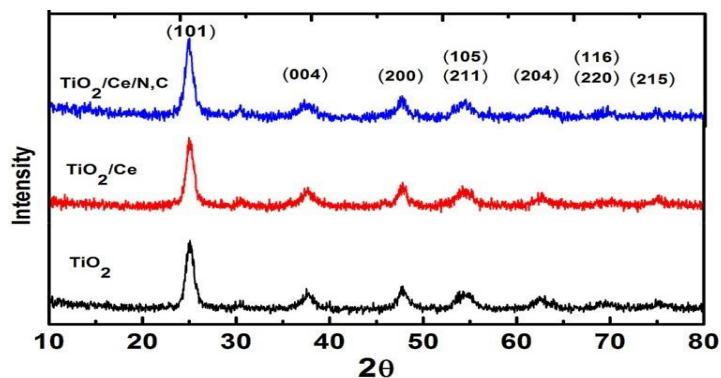


Figure 3: show the XRD pattern of the TiO_2 , TiO_2/Ce , and $\text{TiO}_2/\text{Ce}/\text{N}/\text{C}$.

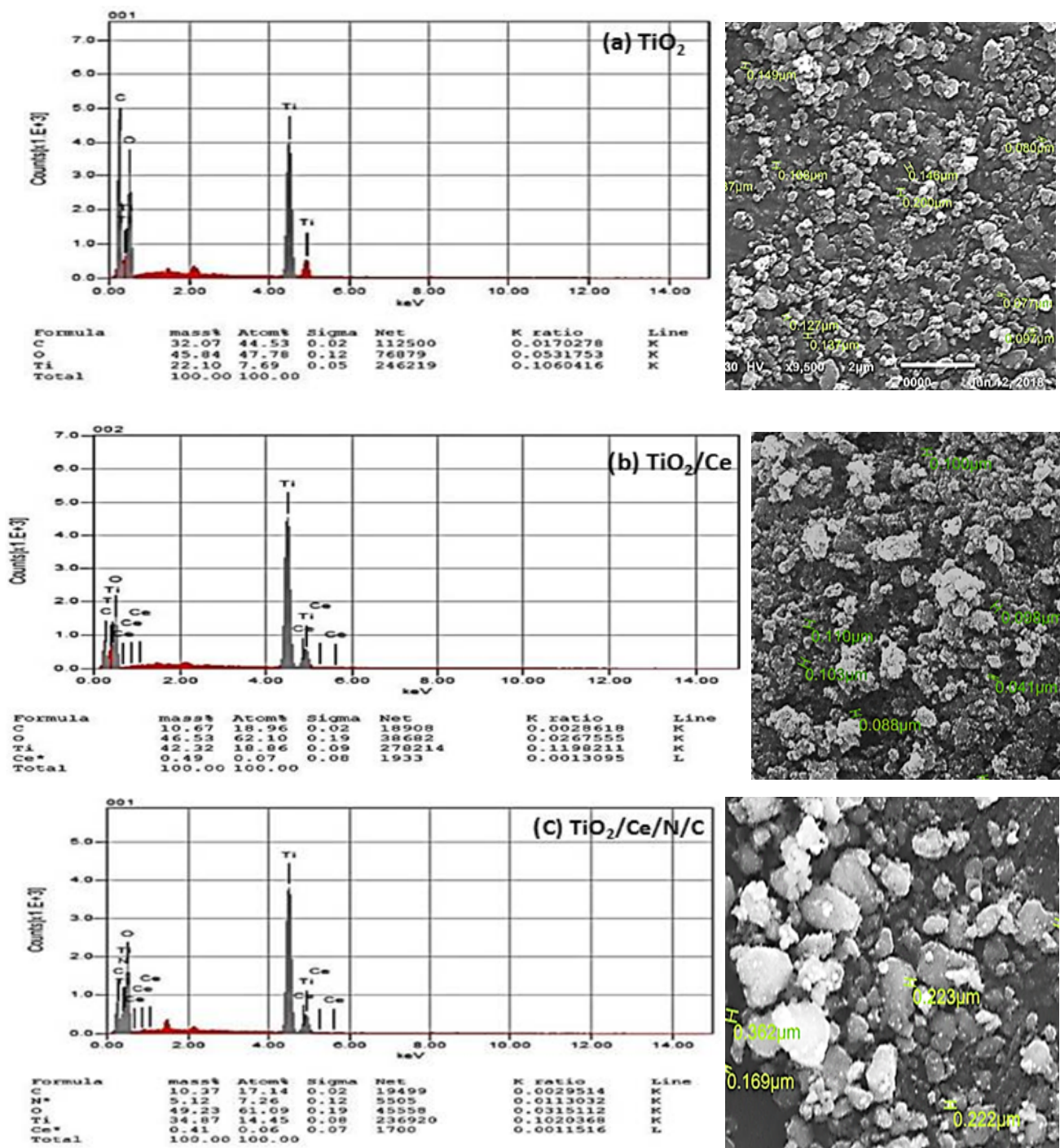


Figure 4: SEM image For (a) TiO_2 , (b) TiO_2/Ce and (c) $\text{TiO}_2/\text{Ce}/\text{N}/\text{C}$

Band gap calculation by UV Spectrophotometer

Calculation of the band gap values for TiO_2 , TiO_2/Ce , and $\text{TiO}_2/\text{Ce}/\text{N}/\text{C}$ nanoparticles was carried out by UV Spectrophotometer. The energy band of the catalyst is the guide of catalytic efficiency. The semiconductor of smaller band gap causes the absorption shift to longer wavelengths in the visible light region, hence more activity and more applicability. The bandgaps of the TiO_2 , TiO_2/Ce and $\text{TiO}_2/\text{Ce}/\text{N}/\text{C}$ were calculated by Kubelka–Munk (KM) method [11] using the following equation(2) :

$$\alpha h\nu = A (h\nu - E_g)^{1/2} \quad (2)$$

Where α , h , ν , E_g , and A are the absorption coefficient, Planck's constant, light frequency, band gap and A is a constant, respectively.

The band gap energy of the TiO_2 , TiO_2/Ce , and $\text{TiO}_2/\text{Ce}/\text{N}/\text{C}$ nanocomposite photocatalysts can be estimated from the intercept of the tangent to the plot of $(\alpha h\nu)^{0.5}$ versus energy ($h\nu$).

From the curves, the band gap was 3.2 e.V and 3.0 e.V for TiO_2 , TiO_2/Ce respectively and decreased to 2.6 e.V for $\text{TiO}_2/\text{Ce}/\text{N}/\text{C}$ and the reflectance spectrum has a redshift. That decreases in the energy gap of heterojunction improving its light absorption properties and enhance visible light applications as its energy is enough to create electron-hole pairs, hence more photocatalytic performance. From the past data of bandgap, it is clear that pure TiO_2 is not applicable in visible light due to large bandgap, so the application was carried out using TiO_2/Ce and $\text{TiO}_2/\text{Ce}/\text{N}/\text{C}$ nanocomposites.

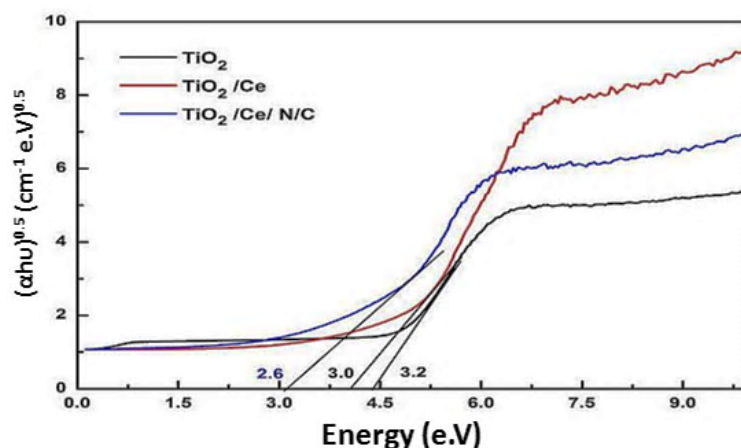


Figure 5: illustrating the decrease in bandgap as a result of catalysts doping

Application:

Our application involves the degradation of the antibacterial drug "metronidazole" in waste water utilizing photocatalytic under the effect of visible light illumination, using the fabricated catalysts TiO_2 , TiO_2/Ce and $\text{TiO}_2/\text{Ce}/\text{N}/\text{C}$.

Degradation of Metronidazole by TiO_2/Ce and $\text{TiO}_2/\text{Ce}/\text{N}/\text{C}$ nanoparticles:

The following graphs prove the enhancement in photoactivity after a composite of TiO_2/Ce by urea to fabricate $\text{TiO}_2/\text{Ce}/\text{N}/\text{C}$ nanocomposite which has better activity. The degradation time of the drug is reduced to a shorter time from 210 min to 120 min.

Kinetic study

The degradation percent [42] was calculated according to the following equation:

$$\text{Photocatalytic degradation \%} = (C_0 - C_t/C_0) \times 100 \quad (3)$$

Where C_0 is the concentration at time zero, C_t is the drug concentration at time t

The photocatalytic reaction kinetics of the fabricated nanocomposites was studied by Langmuir–Hinshelwood standard formula [18]. The expressed equation (4) as follow:

$$\ln(C/C_0) = -K_{app} \cdot t \quad (4)$$

Where C_0 is the concentration at time zero, C is the concentration at time t and K_{app} is the first order reaction constant which is equal to the graph intercept

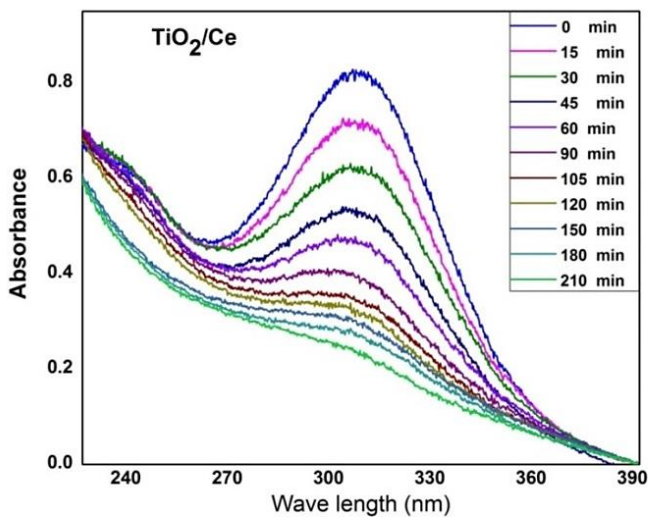


Figure 6: Show the degradation of MTZ with time by TiO_2/Ce

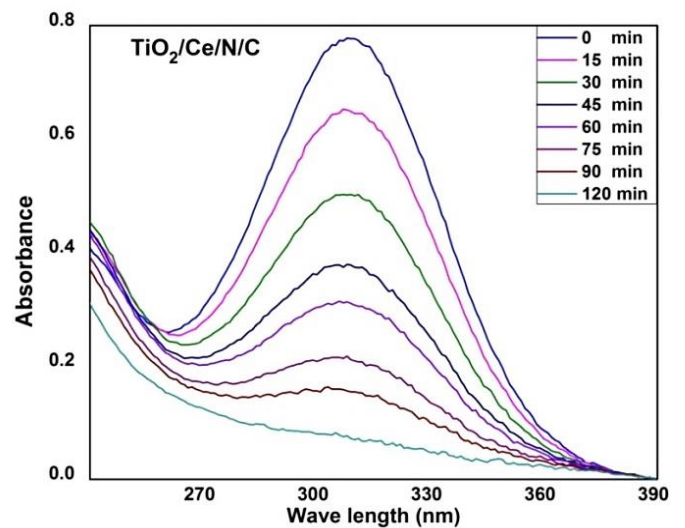


Figure 7: Show the degradation of MTZ with time by $TiO_2/Ce/N/C$

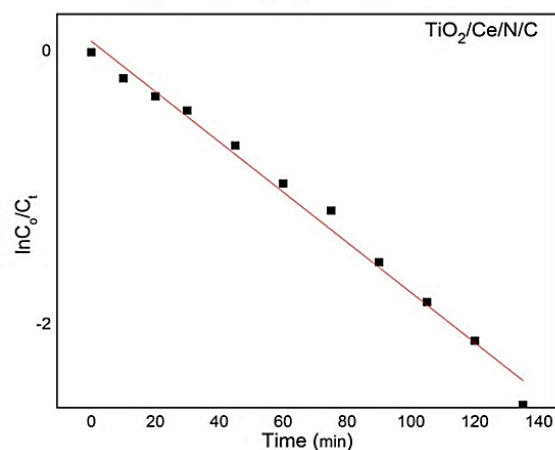
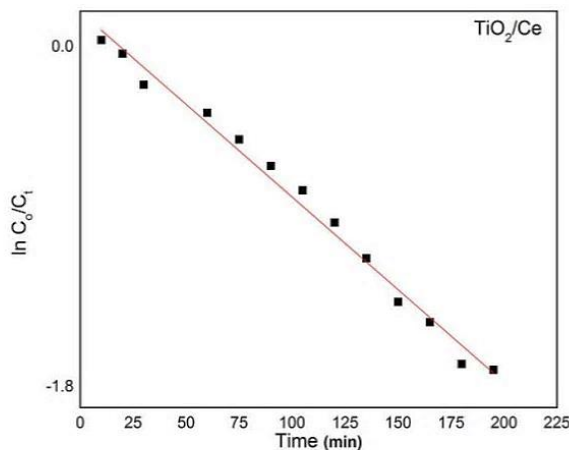


Figure 8: First-order reaction of TiO_2/Ce and $TiO_2/Ce/N/C$ with $k_{app} = 0.19$ and 0.07

For TiO_2/Ce the K_{app} value is 0.19 and 0.07 for $TiO_2/Ce/N/C$ indicating more fitting to first order and more photocatalytic efficiency of $TiO_2/Ce/N/C$.

Conclusion

Preparation of homogenous and small-sized nanoparticles by the sol-gel method is simple, fast and perfect way in nanoparticles synthesis than ordinary methods. Doping of TiO_2 by rare earth metals such as cerium and non-metals like nitrogen and carbon, decrease the band gap to lower value donating better photocatalytic activity to $TiO_2/Ce/N/C$ nanocomposite. The fabricated photocatalyst can actively decompose pharmaceutical compound "metronidazole" from wastewater under the effect of visible light within the reduced time of 120 min only without the need for special procedures

References

1. S. Malato, P. Fernández-Ibáñez, M.I. Maldonado, J. Blanco, W. Gernjak, Decontamination and disinfection of water by solar photocatalysis: recent overview and trends, *Catalysis Today*, 147 (2009) 1-59.
2. A. Längin, R. Alexy, A. König, K. Kümmerer, Deactivation and transformation products in biodegradability testing of β -lactams amoxicillin and piperacillin, *Chemosphere*, 75 (2009) 347-354.
3. K.R. Shoueir, A. Sarhan, A.M. Atta, M.A. Akl, Adsorption studies of Cu^{2+} onto poly (vinyl alcohol)/poly (acrylamide-co-N-isopropylacrylamide) core-shell nanogels synthesized through surfactant-free emulsion polymerization, *Separation Science and Technology*, 51 (2016) 1605-1617.

4. M.A. El-Kemary, I.M. El-mehasseb, K.R. Shoueir, S.E. El-Shafey, O.I. El-Shafey, H.A. Aljohani, R.R. Fouad, Sol-gel TiO₂ decorated on eggshell nanocrystal as engineered adsorbents for removal of acid dye, *Journal of Dispersion Science and Technology*, 39 (2018) 911-921.
5. K. Shoueir, H. El-sheshtawy, M. Misbah, H. El-hosainy, I. El-mehasseb, M. El-kemary, Fenton-like Nanocatalyst for Photodegradation of Methylene Blue under Visible Light Activated by Hybrid Green DNSA@ Chitosan@ MnFe₂O₄, *Carbohydrate Polymers*, (2018).
6. M. Monier, A.L. Shafik, D.A. Abdel-Latif, Synthesis of azo-functionalized ion-imprinted polymeric resin for selective extraction of nickel (II) ions, *Polymer International*, 67 (2018) 1035-1045.
7. R. Hao, X. Xiao, X. Zuo, J. Nan, W. Zhang, Efficient adsorption and visible-light photocatalytic degradation of tetracycline hydrochloride using mesoporous BiOI microspheres, *Journal of hazardous materials*, 209 (2012) 137-145.
8. H.S. El-Sheshtawy, H.M. El-Hosainy, K.R. Shoueir, I.M. El-Mehasseb, M. El-Kemary, Facile immobilization of Ag nanoparticles on g-C₃N₄/V₂O₅ surface for enhancement of post-illumination, catalytic, and photocatalytic activity removal of organic and inorganic pollutants, *Applied Surface Science*, 467 (2019) 268-276.
9. A. Salama, M.A. Diab, R.E. Abou-Zeid, H.A. Aljohani, K.R. Shoueir, Crosslinked alginate/silica/zinc oxide nanocomposite: a sustainable material with antibacterial properties, *Composites Communications*, 7 (2018) 7-11.
10. R. Das, C.D. Vecitis, A. Schulze, B. Cao, A.F. Ismail, X. Lu, J. Chen, S. Ramakrishna, Recent advances in nanomaterials for water protection and monitoring, *Chemical Society Reviews*, 46 (2017) 6946-7020.
11. Z.-L. Shi, C. Du, S.-H. Yao, Preparation and photocatalytic activity of cerium doped anatase titanium dioxide coated magnetite composite, *Journal of the Taiwan Institute of Chemical Engineers*, 42 (2011) 652-657.
12. D.T. Garcia, L.Y. Ozer, F. Parrino, M. Ahmed, G.P. Brudecki, S.W. Hasan, G. Palmisano, Photocatalytic ozonation under visible light for the remediation of water effluents and its integration with an electro-membrane bioreactor, *Chemosphere*, (2018).
13. E.S. Elmolla, M. Chaudhuri, Photocatalytic degradation of amoxicillin, ampicillin and cloxacillin antibiotics in aqueous solution using UV/TiO₂ and UV/H₂O₂/TiO₂ photocatalysis, *Desalination*, 252 (2010) 46-52.
14. P. Calza, V. Sakkas, C. Medana, C. Baiocchi, A. Dimou, E. Pelizzetti, T. Albanis, Photocatalytic degradation study of diclofenac over aqueous TiO₂ suspensions, *Applied Catalysis B: Environmental*, 67 (2006) 197-205.
15. N.M. El-Shafai, M.E. El-Khouly, M. El-Kemary, M.S. Ramadan, A.S. Derbalah, M.S. Masoud, Fabrication and characterization of graphene oxide–titanium dioxide nanocomposite for degradation of some toxic insecticides, *Journal of industrial and engineering chemistry*, 69 (2019) 315-323.
16. N. Okhovat, M. Hashemi, A. Golpayegani, Photocatalytic decomposition of Metronidazole in aqueous solutions using titanium dioxide nanoparticles, *Journal of Materials and Environmental Science*, 6 (2015) 792-799.
17. G. Sauthier, A. Pérez del Pino, A. Figueras, E. György, Synthesis and Characterization of Ag Nanoparticles and Ag-Loaded TiO₂ Photocatalysts, *Journal of the American Ceramic Society*, 94 (2011) 3780-3786.
18. X.-Y. Zhang, H.-P. Li, X.-L. Cui, Y. Lin, Graphene/TiO₂ nanocomposites: synthesis, characterization and application in hydrogen evolution from water photocatalytic splitting, *Journal of Materials Chemistry*, 20 (2010) 2801-2806.
19. N. Yan, Z. Zhu, J. Zhang, Z. Zhao, Q. Liu, Preparation and properties of ce-doped TiO₂ photocatalyst, *Materials Research Bulletin*, 47 (2012) 1869-1873.
20. M.M. Ibrahim, A. Mezni, H.S. El-Sheshtawy, A.A.A. Zaid, M. Alsawat, N. El-Shafi, S.I. Ahmed, A.A. Shaltout, M.A. Amin, T. Kumeria, Direct Z-scheme of Cu₂O/TiO₂ enhanced self-cleaning, antibacterial activity, and UV protection of cotton fiber under sunlight, *Applied Surface Science*, 479 (2019) 953-962.
21. M.H. Misbah, M. Santos, L. Quintanilla, C. Günter, M. Alonso, A. Taubert, J.C. Rodríguez-Cabello, Recombinant DNA technology and click chemistry: a powerful combination for generating a hybrid elastin-like-statherin hydrogel to control calcium phosphate mineralization, *Beilstein journal of nanotechnology*, 8 (2017) 772-783.
22. G. Tian, H. Fu, L. Jing, B. Xin, K. Pan, Preparation and characterization of stable biphasic TiO₂ photocatalyst with high crystallinity, large surface area, and enhanced photoactivity, *The Journal of Physical Chemistry C*, 112 (2008) 3083-3089.
23. M.H. Badr, M. El-Kemary, F.A. Ali, R. Ghazy, Effect of TiCl₄-based TiO₂ compact and blocking layers on efficiency of dye-sensitized solar cells, *Journal of the Chinese Chemical Society*, (2018).
24. A. Bumajdad, M. Madkour, Y. Abdel-Moneam, M. El-Kemary, Nanostructured mesoporous Au/TiO₂ for photocatalytic degradation of a textile dye: the effect of size similarity of the deposited Au with that of TiO₂ pores, *Journal of Materials Science*, 49 (2014) 1743-1754.
25. X. Liu, Y. Gao, C. Cao, H. Luo, W. Wang, Highly crystalline spindle-shaped mesoporous anatase titania particles: solution-phase synthesis, characterization, and photocatalytic properties, *Langmuir*, 26 (2010) 7671-7674.
26. J.H. Pan, X. Zhao, W.I. Lee, Block copolymer-templated synthesis of highly organized mesoporous TiO₂-based films and their photoelectrochemical applications, *Chemical engineering journal*, 170 (2011) 363-380.
27. J.L. Gole, J.D. Stout, C. Burda, Y. Lou, X. Chen, Highly efficient formation of visible light tunable TiO_{2-x}N_x photocatalysts and their transformation at the nanoscale, *The journal of physical chemistry B*, 108 (2004) 1230-1240.
28. M. Montazer, A. Behzadnia, M.B. Moghadam, Superior self-cleaning features on wool fabric using TiO₂/Ag nanocomposite optimized by response surface methodology, *Journal of Applied Polymer Science*, 125 (2012) E356-E363.

29. R. Kato, A. Furube, K.-i. Yamanaka, T. Morikawa, Charge separation and trapping in N-doped TiO₂ photocatalysts: A time-resolved microwave conductivity study, *The Journal of Physical Chemistry Letters*, 1 (2010) 3261-3265.
30. L. Zhao, X. Chen, X. Wang, Y. Zhang, W. Wei, Y. Sun, M. Antonietti, M.M. Titirici, One-step solvothermal synthesis of a carbon@TiO₂ dyade structure effectively promoting visible-light photocatalysis, *Advanced Materials*, 22 (2010) 3317-3321.
31. M.L. Richardson, J.M. Bowron, The fate of pharmaceutical chemicals in the aquatic environment, *Journal of Pharmacy and Pharmacology*, 37 (1985) 1-12.
32. M. Rabølle, N.H. Spliid, Sorption and mobility of metronidazole, olaquinox, oxytetracycline and tylosin in soil, *Chemosphere*, 40 (2000) 715-722.
33. E. Daeseleire, H.D. Ruyck, R.V. Renterghem, Confirmatory assay for the simultaneous detection of penicillins and cephalosporins in milk using liquid chromatography/tandem mass spectrometry, *Rapid communications in mass spectrometry*, 14 (2000) 1404-1409.
34. Z. Fang, X. Qiu, J. Chen, X. Qiu, Degradation of metronidazole by nanoscale zero-valent metal prepared from steel pickling waste liquor, *Applied Catalysis B: Environmental*, 100 (2010) 221-228.
35. W. Cheng, M. Yang, Y. Xie, Z. Fang, J. Nan, P.E. Tsang, Electrochemical degradation of the antibiotic metronidazole in aqueous solution by the Ti/SnO₂-Sb-Ce anode, *Environmental technology*, 34 (2013) 2977-2987.
36. H. Shemer, Y.K. Kunukcu, K.G. Linden, Degradation of the pharmaceutical metronidazole via UV, Fenton and photo-Fenton processes, *Chemosphere*, 63 (2006) 269-276.
37. F. Ingerslev, B. Halling-Sørensen, Biodegradability of metronidazole, olaquinox, and tylosin and formation of tylosin degradation products in aerobic soil-manure slurries, *Ecotoxicology and environmental safety*, 48 (2001) 311-320.
38. J. Liu, G. Zhang, C.Y. Jimmy, Y. Guo, In situ synthesis of Zn₂GeO₄ hollow spheres and their enhanced photocatalytic activity for the degradation of antibiotic metronidazole, *Dalton Transactions*, 42 (2013) 5092-5099.
39. A. Selvaraj, R. Parimiladevi, K. Rajesh, Synthesis of Nitrogen Doped Titanium Dioxide (TiO₂), *J. Environ. Nanotechnol*, 2 (2013) 35-41.
40. Y. Huo, Y. Jin, J. Zhu, H. Li, Highly active TiO₂-x-yN_xF_y visible photocatalyst prepared under supercritical conditions in NH₄F/EtOH fluid, *Applied Catalysis B, Environmental*, 89 (2009) 543-550.
41. S.S. Boxi, S. Paria, Effect of silver doping on TiO₂, CdS, and ZnS nanoparticles for the photocatalytic degradation of metronidazole under visible light, *RSC Advances*, 4 (2014) 37752-37760.
42. D. Yang, Y. Sun, Z. Tong, Y. Tian, Y. Li, Z. Jiang, Synthesis of Ag/TiO₂ nanotube heterojunction with improved visible-light photocatalytic performance inspired by bioadhesion, *The Journal of Physical Chemistry C*, 119 (2015) 5827-5835.

(2019) ; <http://www.jmaterenvironsci.com>